

A Limiting Approach for the Evaluation of Geometric Mean Transmittance in a Multidimensional Absorbing and Isotropically Scattering Medium

W. W. Yuen

Associate Professor,
Department of Mechanical
and Environmental Engineering,
University of California,
Santa Barbara, Calif. 93106
Assoc. Mem. ASME

The calculation of the geometric-mean transmittance factor between areas with an intervening absorbing and isotropically scattering medium is considered. While an exact expression for the factor is shown to be quite complicated, the upper and lower limits of the factor can be readily generated from physical consideration. Integral expressions for successively increasing (decreasing) values of the lower (upper) limits are obtained. For two-dimensional systems, these expressions are reduced to integrals involving $S_n(x)$, a class of exponential integral function that has been tabulated in a previous work. Utilizing the kernel substitution technique, these integrals are evaluated analytically in closed form for some selected geometries. For cases with small optical thickness and large scattering albedo, both limits are shown to converge relatively slowly to the actual transmittance factor. But the decreasing difference between the two limits provides accurate estimate of the geometric-mean transmittance factor. Based on these results, some interesting conclusions concerning the effect of scattering on multidimensional radiative transmission are established.

1 Introduction

The importance of scattering in the analysis of radiative heat transfer in many practical combustion systems is well known [1]. In recent years, significant work has been reported in determining the scattering effect on various radiating systems with simple geometries [2-5].

For practical application, one of the important radiation parameters is the geometric-mean transmittance factor between two arbitrary surfaces. For an intervening medium that is nonparticipating or purely absorbing, the mathematical formulation and method of evaluation for such factors are well known [6, 7]. For an intervening absorbing and scattering medium, however, the amount of reported work is scarce. In their book [6], Hottel and Sarofim estimated the upper and lower limits of the transmissivity and reflectivity of a one-dimensional isotropically scattering slab. In a recent work [8], the present author developed simple analytical expressions for the first approximation of the upper and lower limits of the geometrical-mean transmittance for three selected geometries. These two works, to the best of the present author's knowledge, appear to be the only reported efforts attempting to deal with this difficult problems.

The objective of the present work is to show that by utilizing some simple physical reasoning, the mathematical development presented in [8] can be generalized to yield successively improved estimates of the upper and lower limits of the geometric-mean transmittance factor. Rates of convergence of the two limiting expressions toward the exact value of the transmittance factor are shown to be quite slow for cases with small optical thickness and large scattering albedo. If considered separately, each limiting expression thus has uncertain accuracy in determining the exact transmittance factor. But considered together, the decreasing difference between the two expressions can be used to yield successively

improved approximate values for the transmittance factor and the associated uncertainty. These results are used to assess the effect of scattering on radiative transmission in simple systems. At certain optical thicknesses and scattering albedos, the scattering contribution to the total geometric-mean transmittance factor is shown to be very significant.

2 Analysis

(a) **General Formulation.** For two arbitrary infinitesimal area dA_0 and dA , the energy transfer by radiation from dA_0 to dA can be written as

$$dQ_{dA_0-dA} = q_{o,0} dA_0 dF_{dA_0-dA} (\tau_{dA_0-dA} + \tau_{dA_0-dA}^s) \quad (1)$$

where $q_{o,0}$ is the radiative heat flux leaving surface dA_0 , dF_{dA_0-dA} is the shape factor between dA_0 and dA , τ_{dA_0-dA} is the geometric-mean transmittance between dA_0 and dA calculated only along the line of sight between the two areas, and $\tau_{dA_0-dA}^s$ is the added fraction of energy transfer due to the effect of scattering from elements away from the line of sight. The expression of τ_{dA_0-dA} can be readily obtained from standard reference [6].

In reference [8], first-order approximation for the upper and lower limits of $\tau_{dA_0-dA}^s$ were generated by considering radiative transfer between dA_0 and dA via scattering from a single volume element. Indeed, utilizing a coordinate system as shown in Fig. 1, these limiting expressions are shown to be

$$dF_{dA_0-dA} [\tau_{dA_0-dA}^s]_u = \frac{\sigma}{\pi} \int \int \int \frac{z_1 e^{-EL_1}}{L_1^3} dx_1 dy_1 dz_1 \quad (2)$$

$$dF_{dA_0-dA} [\tau_{dA_0-dA}^s]_l = \frac{\sigma}{4\pi^2} dA$$

$$\int \int \int \frac{z_1 (\mathbf{n} \cdot \mathbf{r}_{1A}) e^{-EL_1 - E_{r1A}}}{L_1 r_{1A}^3} dx_1 dy_1 dz_1 \quad (3)$$

Contributed by the Heat Transfer Division and presented at the ASME-JSME Joint Thermal Engineering Conference, Honolulu, Hawaii, March 1983. Manuscript received by the Heat Transfer Division January 28, 1983.

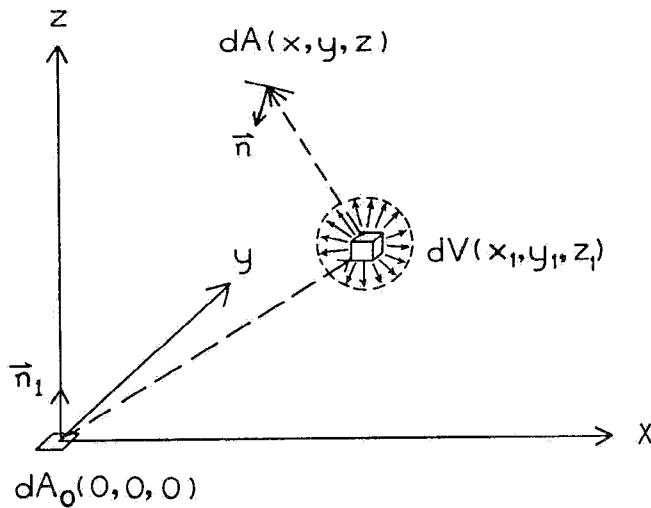


Fig. 1 Coordinate system and geometry for the calculation of the first-order approximation of the geometric-mean transmittance

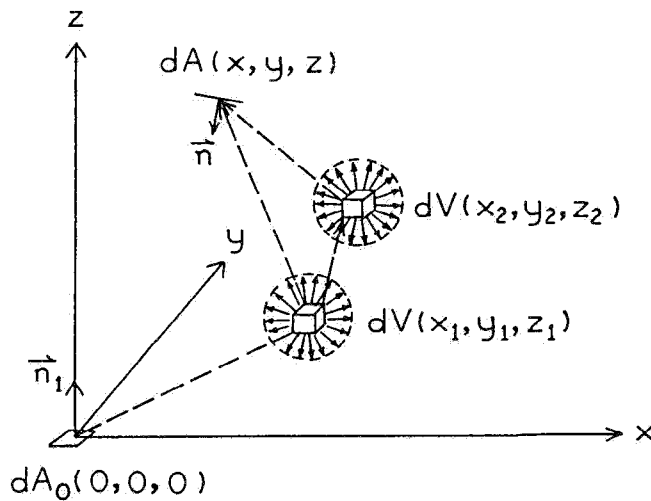


Fig. 2 Coordinate system and geometry for the calculation of the second-order approximation of the geometric-mean transmittance

where

$$E = a + \sigma \quad (4)$$

$$L_1 = (x_1^2 + y_1^2 + z_1^2)^{1/2} \quad (5)$$

and

$$\mathbf{r}_{1A} = (x_1 - x)\hat{i} + (y_1 - y)\hat{j} + (z_1 - z)\hat{k} \quad (6)$$

In the foregoing expressions, dA_0 is assumed to be a diffuse surface; a and σ are the absorption and scattering coefficients of the medium; \hat{i} , \hat{j} , and \hat{k} , unit vectors in the x - y - and z -direction; \mathbf{n} , the unit normal to the surface dA ; and r_{1A} , the magnitude of the vector \mathbf{r}_{1A} . Physically, equation (2) is generated by assuming that all energy scattered by the volume $dx_1 dy_1 dz_1$ will be absorbed by dA . It is clearly the upper limit of τ_{d0-dA}^s . Equation (3), on the other hand, assumes that only the energy scattered from the volume $dx_1 dy_1 dz_1$ in the direction of dA will be absorbed by dA . Since there are always secondary scatterings, equation (3) clearly gives the lower limit of τ_{d0-dA}^s . The limits of integration for equations (2) and (3) generally remain unspecified until the geometry of the scattering medium surrounding dA_0 and dA is defined.

Improved estimates for the upper and lower limits of τ_{d0-dA}^s can be generated by considering physically the added energy transfer between dA_0 and dA due to scattering by multiple volume elements. For example, consider the effect of scattering from two volume elements as shown in Fig. 2. The second-order approximations of the lower and upper limits of τ_{d0-dA}^s can be readily written as

$$dF_{d0-dA} [\tau_{d0-dA}^s]_u^2 = dF_{d0-dA} [\tau_{d0-dA}^s]_l^2 + G_u^2 \quad (7)$$

$$dF_{d0-dA} [\tau_{d0-dA}^s]_l^2 = dF_{d0-dA} [\tau_{d0-dA}^s]_l^2 + G_l^2 \quad (8)$$

where

$$G_u^2 = \frac{\sigma^2}{4\pi^2}$$

$$\int \dots \int \frac{z_1 e^{-E(L_1 + r_{12})}}{L_1^3 r_{12}^2} dx_1 dy_1 dz_1 dx_2 dy_2 dz_2 \quad (9)$$

and

$$G_l^2 = \frac{\sigma^2}{16\pi^3} dA$$

$$\int \dots \int \frac{z_1 (\mathbf{n} \cdot \mathbf{r}_{2A}) e^{-E(L_1 + r_{12} + r_{2A})}}{L_1^3 r_{12}^2 r_{2A}^3} dx_1 dy_1 dz_1 dx_2 dy_2 dz_2 \quad (10)$$

Nomenclature

a = absorption coefficient	M_i = length defined by equation (26)	equations (36), (43) and (56)
A = area	M_{1A} = length defined by equation (23)	x = coordinate
dF = shape factor between differential areas	M_{nA} = length defined by equation (27)	y = coordinate
E = extinction coefficient	n = component of normal vector \mathbf{n} in the z -direction	z = coordinate
F = shape factor	\mathbf{n} = unit normal to area A	σ = scattering coefficient
G = functions defined by equations (15), (16), (24) and (25)	q_o = outgoing radiosity	τ = geometric transmittance factor
\hat{i} = unit vector in x -direction	Q = energy transfer, equation (1)	Subscripts
\hat{j} = unit vector in y -direction	f_{nA} = vector directed from element dA_n to dA	0 = parameter associated with area dA_0
\hat{k} = unit vector in z -direction	$S_n(x)$ = experimental integral function	$d0-dA$ = between area dA_0 and dA
l = component of normal vector \mathbf{n} in the x -direction	U_n = functions defined by equations (32) and (52)	i = coordinates of the i th scattering element
L_1 = length defined by equation (5)	V_n = functions defined by equations (33) and (53)	l = lower limit
L_i = length defined by equation (17)	W_n^m = functions defined by	u = upper limit
M_1 = length defined by equation (22)		Superscripts
		n = order of approximation
		s = scattering contribution

In the above equations, r_{12} and the vector \mathbf{r}_{2A} are given by

$$r_{12} = [(x_1 - x_2)^2 + (y_1 - y_2)^2 + (z_1 - z_2)^2]^{1/2} \quad (11)$$

$$\mathbf{r}_{2A} = (x_2 - x)\hat{i} + (y_2 - y)\hat{j} + (z_2 - z)\hat{k} \quad (12)$$

Physically, G_u^2 represents the radiative energy that is scattered in all direction after scattering by two arbitrary volume elements. It is clearly the maximum amount of energy which can be scattered twice and intercepted by dA . G_l^2 , on the other hand, represents the radiative energy that is scattered in the direction of and intercepted by dA after two scatterings. It is a minimum since energies that are scattered more than twice and intercepted by dA are not included in the consideration.

The foregoing mathematical consideration can be readily generalized to yield successively higher-order approximations of the two limits. Using the same physical argument, it can be readily shown that the n th approximations for the two limits can be written in terms of the $(n-1)$ th approximation by

$$dF_{d0-dA}[\tau_{d0-dA}^s]_u^n = dF_{d0-dA}[\tau_{d0-dA}^s]_{l}^{n-1} + G_u^n \quad (13)$$

$$dF_{d0-dA}[\tau_{d0-dA}^s]_l^n = dF_{d0-dA}[\tau_{d0-dA}^s]_{l}^{n-1} + G_l^n \quad (14)$$

where

$$G_u^n = \left(\frac{\sigma}{\pi}\right) \left(\frac{\sigma}{4\pi}\right)^{n-1}$$

$$\int \dots \int \left(\frac{z_1 e^{-EL_1}}{L_1^3}\right) \left(\prod_{i=2}^{i=n} \frac{e^{-EL_i}}{L_i^2} dx_i dy_i dz_i\right) dx_1 dy_1 dz_1 \quad (15)$$

and

$$G_l^n = \left(\frac{\sigma}{4\pi}\right)^n \frac{dA}{\pi}$$

$$\int \dots \int \frac{z_1 (\mathbf{n} \cdot \mathbf{r}_{nA}) e^{-E(L_1 + r_{nA})}}{L_1^3 r_{nA}^2} \left(\prod_{i=2}^{i=n} \frac{e^{-EL_i}}{L_i^2} dx_i dy_i dz_i\right) dx_1 dy_1 dz_1 \quad (16)$$

In the above expressions, (x_i, y_i, z_i) is the coordinate of the i th scattering volume elements; L_i and \mathbf{r}_{nA} are given by

$$L_i = [(x_i - x_{i-1})^2 + (y_i - y_{i-1})^2 + (z_i - z_{i-1})^2]^{1/2} \quad (17)$$

$$\mathbf{r}_{nA} = (x_n - x)\hat{i} + (y_n - y)\hat{j} + (z_n - z)\hat{k} \quad (18)$$

Physically, it is reasonable to expect that in the limit of $n \rightarrow \infty$, the upper (lower) limit of the scattering contribution to the geometric mean transmittance decreases (increases) monotonically toward the exact value. Mathematically, however, it can be readily shown that the rate of convergence is quite slow. A single limiting expression is thus ineffective in approximating the exact value. Considering both limiting expressions simultaneously, on the other hand, relatively narrow bound of the exact value can be readily generated even with small values of n .

(b) **Two-Dimensional Systems.** For systems with two-dimensional geometry, the foregoing equations can be simplified. Specifically, consider dA to be an infinite strip of width dS with the unit normal \mathbf{n} given by

$$\mathbf{n} = \hat{i} + n\hat{k} \quad (19)$$

equations (1), (13), and (14) still remain valid provided dA_0 and dA are interpreted as infinite stripes. Integrals in the y -direction in equations (2), (3), (9), (10), (15), and (16) can be readily evaluated. As shown in [8], the first-order approximation of the upper and lower limits become

$$dF_{d0-dA}(\tau_{d0-dA}^s)_u^1 = \sigma \int \int \frac{z_1 S_2(EM_1)}{M_1^2} dx_1 dz_1 \quad (20)$$

$$dF_{d0-dA}(\tau_{d0-dA}^s)_l^1 = \frac{\sigma dS}{4}$$

$$\int \int \frac{z_1 [(x_1 - x)l + (z_1 - z)n] S_2(EM_1) S_2(EM_{1A})}{M_1^2 M_{1A}^2} dz_1 dz_1 \quad (21)$$

where

$$M_1 = (x_1^2 + z_1^2)^{1/2} \quad (22)$$

and

$$M_{1A} = [(x_1 - x)^2 + (z_1 - z)^2]^{1/2} \quad (23)$$

Equations (15) and (16) become

$$G_u^n = 4 \left(\frac{\sigma}{4}\right)^n \int \dots \int \frac{z_1 S_2(EM_1)}{M_1^2} \left(\sum_{i=2}^{i=n} \frac{S_1(EM_i) dx_i dz_i}{M_i}\right) dx_1 dz_1 \quad (24)$$

$$G_l^n = \left(\frac{\sigma}{4}\right)^n dS$$

$$\int \dots \int \frac{z_1 [(x_n - x)l + (z_n - z)n] S_2(EM_1) S_2(EM_{nA})}{M_1^2 M_{nA}^2} \left(\sum_{i=2}^{i=n} \frac{S_1(EM_i)}{M_i} dx_i dz_i\right) dx_1 dz_1 \quad (25)$$

where

$$M_i = [(x_i - x_{i-1})^2 + (z_i - z_{i-1})^2]^{1/2} \quad (26)$$

and

$$M_{nA} = [(x_n - x)^2 + (z_n - z)^2]^{1/2} \quad (27)$$

In the foregoing equations, $S_n(x)$ is the exponential integral function, which has been defined and studied extensively in [8] and [9]. Equations (20), (21), (24), (24), together with equations (13) and (14), thus constitute a complete set of mathematical relations, from which the upper and lower limits of τ_{d0-dA}^s can be estimated to an arbitrary order degree of accuracy.

3 Application

In this section, the general mathematical expressions developed in the previous section are applied to three selected geometries to illustrate quantitatively the effect of scattering on the geometric-mean transmittance. The effectiveness of the present approach is also demonstrated. The three cases considered are identical to those studied in [8].

Case 1. In this case, the scattering contribution to the geometric-mean transmittance between dA_0 at the origin and an infinite parallel plane A facing downward toward dA_0 at a given vertical height z is considered. The geometry is shown in Fig. 3(a). The scattering medium is the semi-infinite region below the horizontal plane at z . As in [8], all required integrations are simplified by the introduction of the following kernel substitution

$$S_1(x) = e^{-\frac{\pi x}{2}} \quad (28)$$

$$S_2(x) = \left(\frac{2}{\pi}\right) e^{-\frac{4x}{\pi}} \quad (29)$$

The accuracy of equations (28) and (29) is illustrated in the same reference.

Substituting equations (28) and (29) into equations (24) and (25) and integrating over the following limits

$$\begin{aligned} -\infty < x_i < \infty, & \quad i=1, n \\ -\infty < x < \infty & \\ -\infty < z_i < z, & \quad i=2, n \\ 0 < z_1 < z & \end{aligned}$$

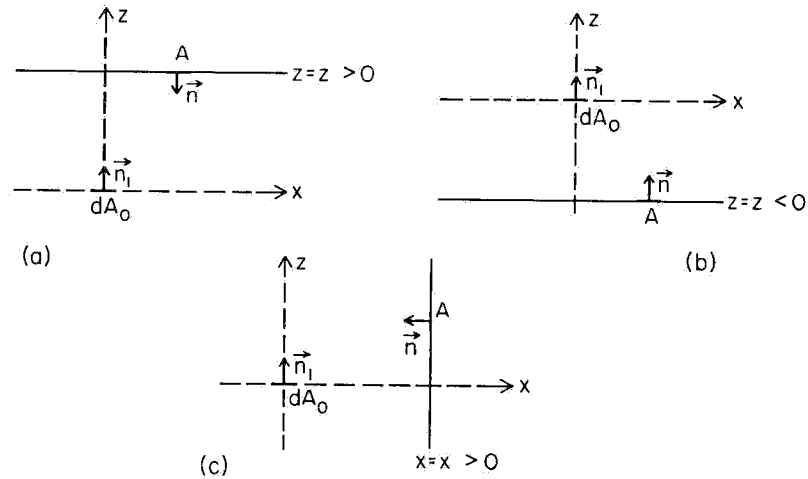


Fig. 3 Geometries of the three specific cases for dA_0 and A considered in the present work

it can be readily shown that G_u^n and G_l^n are readily reduced to

$$G_u^n = 2\sigma \left(\frac{\sigma\pi^2}{8} \right)^{n-1} V_n \quad (30)$$

$$G_l^n = \sigma \left(\frac{\sigma\pi^2}{8} \right)^{n-1} e^{-2Ez} U_n \quad (31)$$

The functions U_n and V_n in the above equations satisfy the following recursive relations

$$U_n = \left[\frac{16}{E(\pi^4 - 64)} \right] \left[\frac{\pi^2}{2} U_{n-1} - \left(\frac{\pi^2 + 8}{4} \right) e^{(2 - \frac{\pi^2}{4})Ez} W_n^0 \right] \quad (32)$$

$$V_n = \left(\frac{4}{\pi^2 E} \right) \left(2V_{n-1} - e^{-\frac{\pi^2}{4}Ez} W_n^0 \right) \quad (33)$$

with

$$U_1 = z \quad (34)$$

and

$$V_1 = \left(\frac{1}{2E} \right) (1 - e^{-2Ez}) \quad (35)$$

The function W_n^m in the above equations is defined by

$$W_n^m = \int \dots \int z_{n-1}^m e^{-E(2z_1 + \frac{\pi^2}{4}z_{n-1})} \left(\prod_{i=2}^{i=n-1} e^{-\frac{\pi^2}{4}E|z_i - z_{i-1}|} dz_i \right) dz_1 \quad (36)$$

For $n = 2$, the above integral can be readily evaluated to yield

$$W_2^m = e^{(\frac{\pi^2}{4} - 2)Ez} \sum_{r=0}^{r=m} (-1)^r \frac{m! z^{m-r}}{(m-r)! \left[\left(\frac{\pi^2}{4} - 2 \right) E \right]^{r+1}} - \frac{(-1)^m m!}{\left[\left(\frac{\pi^2}{4} - 2 \right) E \right]^{m+1}} \quad (37)$$

For $n > 2$, W_n^m can be obtained from the following recursive relation

$$W_n^m = \sum_{r=0}^{r=m} \frac{2(-2)^r m! W_{n-1}^{m-r}}{(m-r)! (\pi^2 E)^{r+1}} + \frac{z^{m+1} W_{n-1}^0 - W_{n-1}^{m+1}}{m+1} \quad (38)$$

From [8], the first-order approximation of the two limits of τ_{d0-A}^s are

$$F_{d0-A}(\tau_{d0-A}^s)_u = \omega(1 - e^{-2Ez}) \quad (39)$$

$$F_{d0-A}(\tau_{d0-A}^s)_l = \omega E z e^{-2Ez} \quad (40)$$

with $\omega = \sigma/E$ being the familiar scattering albedo. Based on equations (39) and (40), and the recursive relations defined by equations (13) and (14), and the expressions for G_u^n and G_l^n as expressed in equations (30-38), the upper and lower limits of the scattering contribution to the geometric-mean transmittance can be readily determined for arbitrary values of n .

Case 2. In this case, A is an infinite parallel plane facing upward at a given location $-z$ as shown in Fig. 3(b). The scattering medium is the semi-infinite region above the horizontal plane at $-z$. Limits of integration become

$$\begin{aligned} -\infty < x_i < \infty, & \quad i=1, n \\ -\infty < x < \infty, & \\ -z < z_i < \infty, & \quad i=2, n \\ 0 < z_1 < \infty & \end{aligned}$$

Direct integration of equations (24) and (25) shows that the generalized relations represented by equations (30-33) remain valid for this geometry. Equations (34-38), however, are replaced by

$$U_1 = \frac{1}{4E} \quad (41)$$

$$V_1 = \frac{1}{2E} \quad (42)$$

$$W_n^m = \int \dots \int z_{n-1}^m e^{-E(2z_1 + \frac{\pi^2}{4}z_{n-1})} \left(\prod_{i=2}^{i=n-1} e^{-\frac{\pi^2}{4}E|z_i - z_{i-1}|} dz_i \right) dz_1 \quad (43)$$

$$W_2^m = \frac{m!}{\left[E \left(\frac{\pi^2}{4} + 2 \right) \right]^{m+1}} \quad (44)$$

$$W_n^m = \sum_{r=0}^{r=m} \frac{2^{r+1} m! W_{n-1}^{m-r}}{(m-r)! (\pi^2 E)^{r+1}} + \frac{z^{m+1} W_{n-1}^0 + W_{n-1}^{m+1}}{m+1} \quad (45)$$

Results in reference [8] yield the following expressions for the lower and upper limits of τ_{d0-A}^s

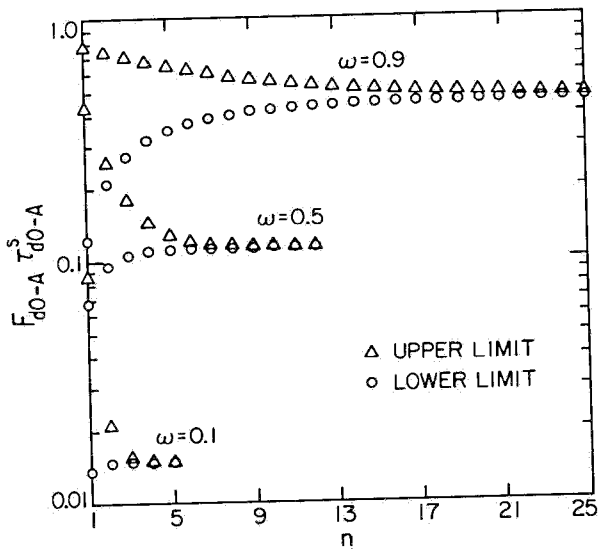


Fig. 4 The convergence behavior of $F_{d0-A} \tau_{d0-A}^s$ for case 1 with $Ez=1.0$

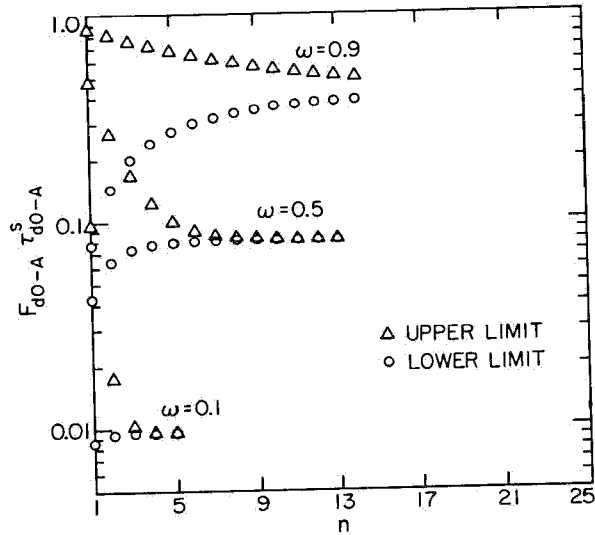


Fig. 6 The convergence behavior of $F_{d0-A} \tau_{d0-A}^s$ for case 3 with $Ex=1.0$

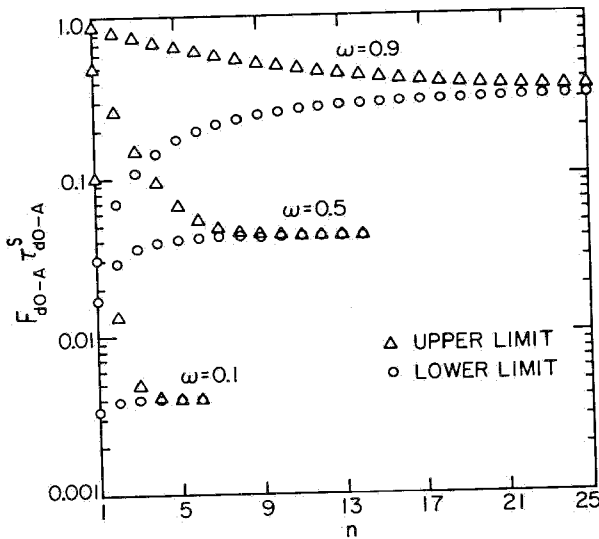


Fig. 5 The convergence behavior of $F_{d0-A} \tau_{d0-A}^s$ for case 2 with $Ez=1.0$

$$F_{d0-A} (\tau_{d0-A}^s)_u = \omega \quad (46)$$

$$F_{d0-A} (\tau_{d0-A}^s)_l = \left(\frac{\omega}{4}\right) e^{-2Ez} \quad (47)$$

Equations (30-33), (41-47), together with equations (13) and (14) can now be used to generate successive approximations for the upper and lower limits of τ_{d0-A}^s for this case.

Case 3. In this case, A is an infinite vertical plane facing the origin at a given location z as shown in Fig. 3(c). The scattering medium is the semi-infinite region to the left of the vertical plane at x . Limits of integration for this case become

$$\begin{aligned} -\infty < x_i < x, & \quad i=1, n \\ -\infty < z < \infty & \\ -\infty < z_i < \infty, & \quad i=2, n \\ 0 < z_1 < \infty & \end{aligned}$$

As shown in [8], additional kernel substitutions for the regular exponential functions $E_1(x)$ and $E_2(x)$ are required before integrals as represented by equations (24) and (25) can be evaluated in closed form. These substitutions are

$$E_1(x) = 2e^{-2x} \quad (48)$$

$$E_2(x) = e^{-2x} \quad (49)$$

After integrations, a set of equation analogous to equations (30-40) are generated. They are

$$G_l^n = \frac{4\sigma}{\pi} \left(\frac{\sigma\pi^2}{8}\right)^{n-1} V_n \quad (50)$$

$$G_l^n = \frac{2\sigma}{\pi} \left(\frac{\sigma\pi^2}{8}\right)^{n-1} e^{-2Ex} U_n \quad (51)$$

$$U_n = \left[\frac{16}{E(\pi^4 - 64)} \right] \left[\frac{\pi^2}{2} U_{n-1} - \left(\frac{\pi^2 + 8}{4}\right) e^{(2 - \frac{\pi^2}{4})Ex} W_n^0 \right] \quad (52)$$

$$V_n = \left(\frac{4}{\pi^2 E}\right) \left(2V_{n-1} - e^{-\frac{\pi^2}{4}Ex} W_n^0\right) \quad (53)$$

$$U_1 = \left[\frac{\pi}{2E(\pi - 4)} \right] \left(e^{(2 - \frac{8}{\pi})Ex} - \frac{8}{4 + \pi} \right) \quad (54)$$

$$V_1 = \left(\frac{\pi}{4E}\right) \left(1 - \frac{e^{-\frac{8}{\pi}Ex}}{2}\right) \quad (55)$$

$$W_n^m = \int \dots \int x_1^m e^{\frac{\pi^2}{4}Ex_{n-1}} e^{-\frac{8}{\pi}E|x_1|} \left(\sum_{i=2}^{i=n-1} e^{-\frac{\pi^2}{4}E|x_i - x_{i-1}|} dx_i \right) dx_1 \quad (56)$$

$$W_2^m = e^{\left(\frac{\pi^2}{4} - \frac{8}{\pi}\right)Ex} \sum_{r=0}^{r=m} (-1)^r \frac{m! x^{m-r}}{(m-r)! \left[\left(\frac{\pi^2}{4} - \frac{8}{\pi}\right)E\right]^{r+1}} - (-1)^m m! \left[\frac{1}{\left[\left(\frac{\pi^2}{4} - \frac{8}{\pi}\right)E\right]^{m+1}} - \frac{1}{\left[\left(\frac{\pi^2}{4} + \frac{8}{\pi}\right)E\right]^{m+1}} \right] \quad (57)$$

$$W_n^m = \sum_{r=0}^{r=m} \frac{2(-2)^r m! W_{n-1}^{m-r}}{(m-r)! (\pi^2 E)^{r+1}} + \frac{x^{m+1} W_{n-1}^0 - W_{n-1}^{m+1}}{m+1} \quad (58)$$

COLORADO STATE UNIVERSITY

Table 1 Values of the upper and lower limits of $F_{d0-A} \tau_{d0-A}^s$ for case 1 (n is the order of approximation used in generating the presented values)

$Ez(F_{d0-A} \tau_{d0-A})$	ω	n	$F_{d0-A}(\tau_{d0-A}^s)_l$	$F_{d0-A}(\tau_{d0-A}^s)_u$
0.1(0.8326)	0.1	5	0.8479e-2	0.8479e-2
	0.5	12	0.5062e-1	0.5062e-1
	0.9	25	0.1285	0.1302
0.5(0.4432)	0.1	5	0.1950e-1	0.1950e-1
	0.5	13	0.1304	0.1304
	0.9	25	0.4035	0.4122
1.0(0.2194)	0.1	5	0.1472e-1	0.1472e-1
	0.5	12	0.1125	0.1126
	0.9	25	0.4518	0.4696
2.0(0.0602)	0.1	5	0.4155e-2	0.4156e-2
	0.5	9	0.4071e-1	0.4075e-1
	0.9	25	0.2890	0.0329

Table 2 Values of the upper and lower limits of $F_{d0-A} \tau_{d0-A}^s$ for case 2 (n is the order of approximation used in generating the presented values: note that $F_{d0-A} \tau_{d0-A}^s$ is zero for this case)

Ez	ω	n	$F_{d0-A}(\tau_{d0-A}^s)_l$	$F_{d0-A}(\tau_{d0-A}^s)_u$
0	0.1	5	0.2648e-1	0.2648e-1
	0.5	11	0.1779	0.1781
	0.9	25	0.5782	0.5955
0.1	0.1	5	0.2192e-1	0.2193e-1
	0.5	12	0.1552	0.1553
	0.9	25	0.5490	0.5682
0.5	0.1	5	0.1025e-1	0.1026e-1
	0.5	13	0.8803e-1	0.8809e-1
	0.9	25	0.4320	0.4585
1.0	0.1	6	0.3928e-2	0.3929e-2
	0.5	14	0.4182e-1	0.4186e-1
	0.9	25	0.3059	0.3407
2.0	0.1	7	0.5647e-3	0.5648e-3
	0.5	17	0.8761e-2	0.8767e-2
	0.9	25	0.1424	0.1911

Table 3 Values of the upper and lower limits of $F_{d0-A} \tau_{d0-A}^s$ for case 1 (n is the order of approximation used in generating the presented values)

$Ex(F_{d0-A} \tau_{d0-A})$	ω	n	$F_{d0-A}(\tau_{d0-A}^s)_l$	$F_{d0-A}(\tau_{d0-A}^s)_u$
0(0.5000)	0.1	5	0.1478e-1	0.1479e-1
	0.5	11	0.9759e-1	0.9766e-1
	0.9	13	0.2963	0.3333
0.1(0.3480)	0.1	5	0.1749e-1	0.1749e-1
	0.5	11	0.1166	0.1167
	0.9	13	0.3600	0.4059
0.5(0.1409)	0.1	5	0.1660e-1	0.1661e-1
	0.5	12	0.1216	0.1217
	0.9	13	0.4408	0.5231
1.0(0.5822e-1)	0.1	5	0.9447e-2	0.9454e-2
	0.5	13	0.7974e-1	0.7980e-1
	0.9	14	0.3771	0.4558
2.0(0.1203e-1)	0.1	6	0.1948e-2	0.1949e-2
	0.5	15	0.2204e-1	0.2206e-1
	0.9	15	0.1920	0.3368

$$F_{d0-A}(\tau_{d0-A}^s)_u = \frac{\omega}{2} \left(2 - e^{-\frac{8}{\pi} Ex} \right) \quad (59)$$

$$F_{d0-A}(\tau_{d0-A}^s)_l = \left(\frac{\omega}{4 - \pi} \right) \left(\frac{8e^{-2Ex}}{4 + \pi} - e^{-\frac{8}{\pi} Ex} \right) \quad (60)$$

4 Results and Discussion

The rate of convergence of the present approach in determining the actual scattering contribution of the geometric-mean transmittance is illustrated for the three cases in Figs. 4, 5, and 6. Since G_u^n and G_l^n are both proportional to σ^n (and consequently to ω^n) as shown in equations (50) and

(51), the upper and lower limits of the geometric mean transmittance is a polynomial in ω of order n at the n th approximation. Cases with small scattering albedo thus converge relatively quickly. The general behavior of the numerical results for different optical thickness is similar to those presented in these figures. The rate of convergence general decreases with increasing optical thickness. For cases 1 and 2, evaluations of the two limits are carried out only up to $n = 25$. At $n > 25$, numerical results show that the difference between successive approximations is smaller than the accuracy of the computer. The higher-order results for these two cases are thus meaningless. For case 3, the two limiting solutions begin to oscillate as n becomes large. This behavior

is probably due to the error of the kernel substitution. The computation is thus stopped at the lowest value of n beyond which this oscillation occurs.

In spite of the foregoing limitations, the present results show clearly that the effect of scattering is extremely important and cannot be ignored in any realistic engineering calculation involving radiative transfer. The best estimates of the two limits of the scattering contribution to the geometric mean transmittance for the three cases are presented in Tables 1, 2, and 3. Geometric mean transmittances without the scattering contribution are presented in these same Tables for comparison. In all three cases, it can be readily observed that for cases with intermediate or large scattering albedo ($\omega > 0.5$), scattering is the major contribution to the geometric transmittance. Neglecting scattering in these cases can lead to errors ranging from 6 percent ($\omega = 0.5$, $Ez = 0.1$ in case 1) to 1000 percent ($\omega = 0.9$, $Ex = 2.0$ in case 3). In case 2, in fact, scattering represents the only contribution to the geometric transmittance function. The effect of scattering also appears to be most dominant for cases with intermediate optical thickness.

Finally, it is interesting to observe that the geometry in case 2, with $Ez = 0$, can be considered as an approximation of a burning fuel bed. Results in Table 2 show that the amount of radiation reabsorbed by a fuel bed enclosed by a scattering medium (such as the flame) can be as high as 60 percent. Because of the presence of soot and other products of incomplete combustion, the scattering albedo for most combusting media is not small. The present results clearly demonstrate that any energy balance calculations for such fuel beds without including the effect of scattering can be in substantial error.

5 Conclusion

An approach is developed to evaluate the upper and lower limits of the geometric mean transmittance between surfaces

with an intervening absorbing and scattering medium. Explicit analytical expressions are generated for three systems with two-dimensional geometry. Results show that for such systems, the effect of scattering is extremely important and in some cases constitutes the dominant effect in radiative transfer. An interesting result concerning the reabsorption by a burning fuel bed is also generated.

Acknowledgment

This paper is based upon work supported by the National Science Foundation, Grant No. MEA80-24824.

References

- 1 de Ris, J., "Fire Radiation, A Review," *The Seventeen Symposium (International) on Combustion*, The Combustion Institute, 1978, pp. 1003-1016.
- 2 Crosbie, A. L., and Linsenbardt, T. L., "Two-Dimensional Isotropic Scattering in a Semi-Infinite Medium," *Journal of Quantitative Spectroscopy and Radiative Transfer*, Vol. 19, 1978, pp. 257-284.
- 3 Dolin, L. S., "Propagation of a Narrow Beam of Light in a Medium With Strongly Anisotropic Scattering," *Soviet Radiophysics*, Vol. 9, 1966, pp. 40-47.
- 4 Lee, H., and Buckius, R. O., "Scaling Anisotropic Scattering in Radiation Heat Transfer for a Planar Medium," *ASME JOURNAL OF HEAT TRANSFER*, Vol. 104, 1982, pp. 68-75.
- 5 Goswami, D. Y., and Vachou, R. I., "Radiative Heat Transfer Analysis Using an Effective Absorptivity for Absorption, Emission, and Scattering," *International Journal of Heat and Mass Transfer*, Vol. 20, 1977, pp. 1233-1239.
- 6 Hottel, H. C., and Sarofim, A. F., *Radiative Transfer*, McGraw Hill, New York, 1967.
- 7 Yuen, W. W., "A Simplified Approach to the Evaluation of Geometric-Mean Transmittance and Absorption for Gas Enclosure," *ASME JOURNAL OF HEAT TRANSFER*, Vol. 102, 1981, pp. 88-813.
- 8 Yuen, W. W., "Evaluation of Geometric-Mean Transmittance Factor in Multidimensional Absorbing and Isotropically-Scattering Media," *Proceeding of The 1983 ASME/JSME Thermal Engineering Joint Conference*, Vol. 4, 1983, pp. 27-32.
- 9 Yuen, W. W., and Wong, L. W., "Numerical Computation of an Important Integral Function in Two-Dimensional Radiative Transfer," *The Journal of Quantitative Spectroscopy and Radiative Transfer*, Vol. 29, No. 2, 1983, pp. 145-149.